# Chapter 2
# Digital Fabrication with Cement-Based Materials: Process Classification and Case Studies


**R. A. Buswell, F. P. Bos, Wilson Ricardo Leal da Silva, N. Hack, Harald Kloft, Dirk Lowke, Niklas Freund, Asko Fromm, E. Dini, Timothy Wangler, E. Lloret-Fritschi, Roel Schipper, Viktor Mechtcherine, Arnaud Perrot, K. Vasilic, and Nicolas Roussel**

**Abstract** The need for methods for forming concrete has existed for as long as concrete has been used in constructing the built environment. Creating flat, rectilinear formers have traditionally been the cost and time efficient default for the majority of applications. The desire for greater design freedom and the drive to automate construction manufacturing is providing a platform for the continued development of a family of processes called Digital Fabrication with Concrete

R. A. Buswell (✉)
School of Architecture, Building and Civil Engineering, Loughborough University, Loughborough, UK
e-mail: r.a.buswell@lboro.ac.uk

F. P. Bos
Department of the Built Environment, Eindhoven University of Technology, Eindhoven, Netherlands

W. R. L. da Silva
Danish Technological Institute, Taastrup, Denmark

N. Hack · H. Kloft
Institute of Structural Design, Technische Universitat Braunschweig, Braunschweig, Germany

D. Lowke · N. Freund
Institute of Building Materials, Concrete Construction and Fire Safety, Technische Universitat Braunschweig, Braunschweig, Germany

A. Fromm
Hochschule Wismar. University of Applied Sciences, Technology, Business and Design—structural design, Wismar, Germany

E. Dini
Monolite Ltd, 101 Wardour Street, London W10UN, UK

T. Wangler · E. Lloret-Fritschi
Institute for Building Materials, Physical Chemistry of Building Materials, ETH Zurich, Zurich, Switzerland

R. Schipper
Department Materials, Mechanics, Management & Design, Delft University of Technology, Delft, Netherlands



N. Roussel and D. Lowke (eds.), *Digital Fabrication with Cement-Based Materials*,
RILEM State-of-the-Art Reports 36, https://doi.org/10.1007/978-3-030-90535-4_2

(DFC) technologies. DFC technologies are many and varied. Much of the material science theory is common, but the process steps vary significantly between methods, creating challenges as we look towards performance comparison and standardisation. Presented here is a framework to help identify and describe process differences and a showcase of DFC application case studies that explain the processes behind a sub-set of the technologies available.

## 2.1 Introduction

Productivity, cost overruns and quality in the construction sector has for many years been a recognised problem (Latham 1994; Egan 1998). Productivity in particular has stagnated over the last 25 years, compared to almost doubling in other sectors (Changali et al. 2015). Automation and the digitisation of information exchange, communication and control are expected to play a key role in helping to mitigate these issues (Barbosa et al. 2017; Siemens 2017; HMGoverment 2017). While innovation in construction machines is not new (Urshel 1941), automation presents a significant departure from conventional construction methods. Historically, the application of robotics has been of significant interest (Kuntse et al. 1995; Yamazaki and Maeda 1998; Gambao et al. 2000).

Digital Fabrication with Concrete (DFC) methods are a family of technologies that offer digital control over the design and manufacturing process (Buchi et al. 2018; Buswell et al. 2020). They promise the manufacture of both architectural and structural components (Hack et al. 2013; Labonnote et al. 2016; Buswell et al. 2018; Aspone et al. 2018; Mechtcherine et al. 2019) and have been the focal point for significant development in the field of cement-based mortars, particularly with respect to the hardened properties (Le et al. 2012a; Nerella et al. 2019; Tay et al. 2019); control and understanding of rheology (Le et al. 2012b; Roussel 2018); control of structural build-up and on-demand setting (Reiter et al. 2018; Marchon et al. 2018); and the mechanics of the building up layers of wet material without formwork (Wolfs 2018a, 2019a).

DFC methods have been around for some time with its roots in Computer Numeric Control (CNC), which took hold in the 1960s. CNC developed through the 1970 and 1980s where the computer revolution initiated the development of computer-aided

V. Mechtcherine
Institute of Construction Materials, Technische Universitat Dresden, Dresden, Germany

A. Perrot
Univ. Bretagne Sud, UMR CNRS 6027, IRDL, 56100 Lorient, France

K. Vasilic
German Society for Concrete and Construction Technology, Berlin, Germany

N. Roussel
Laboratoire Navier, Gustave Eiffel University, Eiffel, France

design software that allows for 'parametric' design (Howe 2000; Schodek et al. 2005; Menges 2006). These tools have driven architectural design for many years and the construction of Frank Gehry's Zollhoff Towers in Dusseldorf (2000) which was modelled in CATIA, and used CNC cutting and milling to generate foam moulds used to cast the structure of the building, is just one example (Kolarevic 2005).

In the product design field, the computer-aided design (CAD) environment allowed for the digital design of products; however, a prototype model for aesthetic and/or functional testing needed to be carried out by hand. In the 1980s, the first layer-based manufacturing process emerged that made it possible for a physical model to be created directly from CAD data. This significantly reduced the cycle time for evaluating product prototypes, and Rapid Prototyping was established (Lipson and Kurman 2013).

Over the last 25 years, there have been considerable developments in materials. The use of these *Rapid Prototyping* machines for the production of end-use parts has developed into *Additive Manufacturing* (Gibson et al. 2015). The flexibility in the geometries that could be produced led to early actors exploring similar principles to create large architectural components (Lim et al. 2012). However, additive approaches are just one process type in the DFC family and moulding systems such as TailorCrete (Andersen et al. 2016) and Smart Dynamic Casting (Lloret-Fritschi 2020) are just two examples of alternative methods.

The contemporary field is becoming populated with many actors internationally, both commercial and academic, and there is a terrific variety in the materials and processes used. Indeed, there is a significant variation in system maturity and in the manufacturing applications under investigation. The configuration of mixing and pumping, the use of admixtures, the mortar/concrete composition and the design of what is being manufactured all affect the process design and the criticality of operational parameters. The comparison of the performance of two systems as well as the quality of the material produced by them is, therefore, challenging.

Recognising the need to clearly understand and articulate the differences between DFC processes, and thus allow performance comparison and the initiation of standardisation, the RILEM TC-276 undertook to develop a classification framework for DFC. This has been recently published and provides an overview of classification methods, developing the state of the art into a set of principles and an approach to allow the unambiguous definition and description of a DFC process (Buswell et al. 2020). The work is published under an open access agreement. This chapter describes the above classification framework and is followed by a series of DFC application case studies that illustrate the differences in practice.

## 2.2 Assembly and Material Forming Processes

Buildings, like cars, are complex assemblies comprising of parts (windscreen in a car/window in a building) and sub-assemblies (the engine in a car/an air-conditioning chiller in a building). These require the design and manufacture of many components, using different shaping processes, dictated by the material characteristics and the

form required. The complexity of the form will limit what is achievable in a single component, compare a plastic spoon to the bodywork on a car, or the façade of a building. Individual parts, therefore, need to be assembled to produce the whole product, and that assembly requires the joining of adjacent parts.

Permanent *joining* can be achieved using methods such as *welding/brazing* and *soldering/adhesives*, or through the application of permanent fasteners (snap-fits is one example, (Troughton 2009)). Welding uses energy to melt the material, typically metals and thermoplastics, to create a pool of material which then cools joining parts through fusion. There are many sub-classes of welding, of which two are Gas Metal Arc (MIG) and Electron Beam. Brazing and soldering use a second material that is melted to join two parts, rather than melting the part material: the temperature, at which the filler material melts, determines which name is used. Adhesives use a chemical bonding process. There are many examples of these methods in all industries and to pick two within DFC: MeshMould utilises welding to permanently assemble a reinforcement cage (Hack et al. 2020), the Fastbrick (Bonwetsch 2015) utilises adhesive bonding to join bricks. When components need to be removed for maintenance, replacement, or disassembly at the end of life, temporary fastenings may be deployed where screws, nuts and bolts are examples of *threaded fasteners*.

Parts can require *surface treatment*, *coating*, or other deposition processes to achieve a particular function, often to increase durability or provide an aesthetic finish. Examples in metals are case-hardening, through diffusion or heat treatments and in concrete, include hydrophobic impregnation. Painting is a common coating throughout manufacturing and construction that provides protection of the material from the environment in addition to providing aesthetic options.

The production of the individual parts themselves requires the shaping of material, which can be achieved using either *formative*, *additive* or *subtractive* processes. Formative methods shape a finite volume of material using a preformed mould, die or surface. Approaches that rely on the *solidification* of material use a mould into which the fluid material is poured, or injected. The forces required to take on the shape of the form depend on the material properties: being driven by gravity in the conventional casting of concrete, or under high-pressure in injection moulding, for example. *Deformation* approaches rely on the plastic state of the material and include methods such as stamping, rolling and pressing. DFC processes such as Smart Dynamic Casting (SDC, Sect. 2.4.6) and Adapta (Sect. 2.4.7) rely on the plastic state of concrete/cement-based mortar.

Subtractive methods shape the desired geometry from a larger volume of material, that is cut, drilled, milled and ground away until the form is realised. Examples include stone masonry, sculpture or turning items on a lathe or other CNC tool. In DFC, milling or hot wire cutting is commonly used to create bespoke moulds (Garcia 2010). Additive Manufacturing, however, is the inverse where material is progressively placed until the final form has been created. ISO 17296 2015, 2016 recognise seven additive process classes, of which the three that are commonly found in manufacturing and DFC are: *material extrusion* (Fuse Deposition Modelling, 3D concrete printing, i.e. Sects. 2.4.1, 2.4.2, 2.4.3, and 2.4.8); *material jetting* (Thermojet, Shotcrete 3D concrete printing, Sect. 2.4.4); and Binder Jetting (3D

Systems ZPrinter) which is often referred to as *Particle-bed Binding* in construction applications (Sect. 2.4.5). Further details on Additive Manufacturing can be found in Gibson et al. (2015).

## 2.3 Classification of DFC Processes

The full details of the classification framework are presented in Buswell et al. (2020), which is an open access publication. In principle, it should:

- encompass the broad spectrum of processes found in DFC;
- maintain differentiation between on-site, in-situ processes and processes for the production of parts in a factory;
- be based on pre-existing definitions and commonly understood frameworks of material forming and assembly processes; and,
- seek to build on (or adopt) existing standards where practicable.

Within the board DFC family, the material used is similar in so far as the binding agent belongs to the family of cements with related properties, and these are often combined with aggregates to form a mortar or concrete material. DFC process are typically designed and tested to manufacture a famility of cement based products: such as panels, or walls, or columns. These applications tend to inform the selection of critical process and material parameters (Buswell et al. 2018).

Once these requirements are identified, additional processes are employed to affect particular operations, which could be surface smoothing, in the case of Contour Crafting (Khoshnevis 2006), hydration control when the objects under manufacture need to be rapidly built in the vertical direction (Gosselin 2016), or the assembly of the reinforcement mesh prior to casting in the MeshMould application (Hack and Lauer 2014). A closer inspection of the technology, reveals yet more sub-processes that could incorporate automated measurement such as that used to control deposition height through real-time feedback control (Wolfs et al. 2018b) or the mixing and pumping of mortars (in almost all processes) for example.

These sub-processes are often required to enable the main material forming process to take place, and so with the intent to create a meaningful classification method, we find that we can distinguish the processes based on the primary material forming process, for which frameworks exist. However, we must take care to clearly identify sub-process to either differentiate methods or identify those that are effectively equivalent.

It can also be helpful to consider the operations involved in manufacture against a notional time scale where processes may be found to operate in series (one after the other in relative isolation, where a formwork might be printed and subsequently used for forming cast material), simultaneously (where they happen at the same time, wire reinforcement for example (Asprone et al. 2018), or contiguously where processes alternate at repeated stages in a process, such as the addition of a support material

in an additive manufacturing process). An approach to visualising these interactions using 'process sketches' is given in Buswell et al. (2020).

In addition to defining the nature of the process boundaries, implementation and sequencing, it is useful to identify the *Material*, and, with concrete and mortars, we are referring to the mix design as these vary significantly. The (intended) *Application* environment is also important, and this is principally whether it is for off-site or on-site use, since environmental factors play a significant role in the process operation and success. Next, the *Product* under manufacture also affects the *Process* as does size and mass: for example, the requirements for the set control for the production of vertical walls is significantly different from a thin horizontal panel, as is using DFC to manufacture a formwork for casting or to create solid end-use components with additive processes directly (Buswell et al. 2018). These form the so-called *MAPP (Material-Application-Product-Process)* definitions that delimit the suggested classification allowing the clear communication of a specific implementation of DFC technology.

Figure 2.1 presents the classification framework, which largely follows a conventional manufacturing view of assembly and shaping processes (adapted from Grover 2012) and includes surface treatments. As long as the boundaries of the process are well defined, most DFC processes will fall into this classification. Care needs to be taken in order that the object and purpose of the process is not conflated. For example: milling of a foam former is a subtractive DFC method, applied to form polystyrene—the product being a mould, which is part of a two-step process, in which a second step is to cast the actual part.

Additive Manufacturing processes fall outside conventional manufacturing and have a second tier of classification as part on (ISO 17296: 2015 and 2016) and these are reflected here with the exception that 'binder jetting' has been replaced with the term 'particle-bed binding'. The approach is readily extensible if/when other process types emerge. In the following section, eight case study applications with different processes are presented that cover a significant proportion of the classes presented.

## 2.4 Case Studies

Eight case studies are presented here. They represent different application environments, materials, products and processes, covering a good proportion of the classification framework pictured in Fig. 2.1. These case studies illustrate the key differences between the processes used, thus providing a context for Chaps. 3 to 6 in this book. Table 2.1 provides an overview of the MAPP definition (Buswell et al. 2020) for each of the case studies. Although some technologies are used to manufacture the same products, or hold the same process classification, note that the combination of main forming process (on which the classification is based) and essential sub-processes is different in every case.

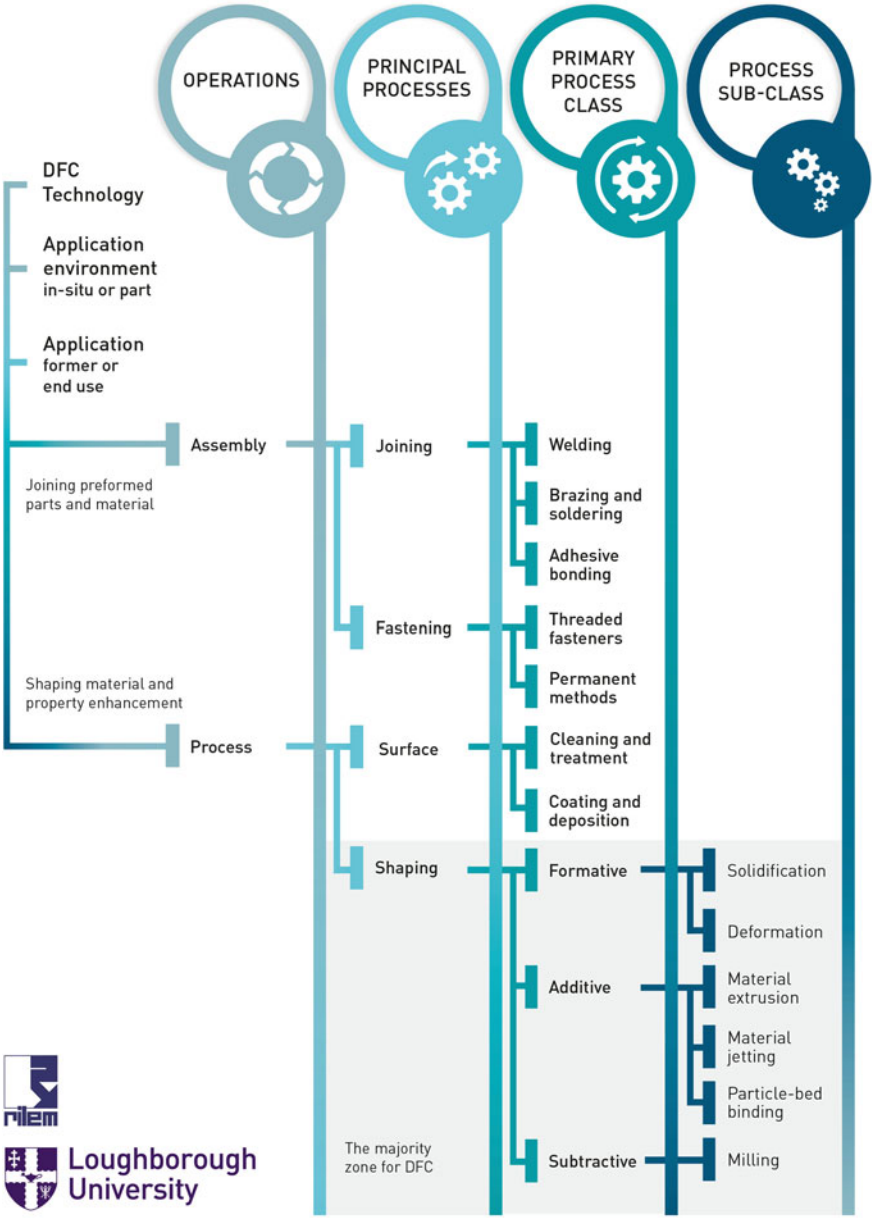


**Fig. 2.1** A process classification framework for Digital Fabrication with Concrete, indicating the majority zone in which most DFC processes reside (Buswell et al. 2020)

**Table 2.1** The MAPP definition for each case study

| Case Study | Material | Application | Product | Process (Classification) | Sub-processes | Organisation | Country |
|---|---|---|---|---|---|---|---|
| 1 | Wet mix, cement mortar <1 mm | Off-site production | Printing and assembling a 6.5 m Bicycle Bridge | Additive manfacturing: Material Extrusion | Insertion of wire reinforcement in the extruded filament | TU Eindhoven | Natherlands |
| 2 | Wet mix, cement mortar <2 mm | Off-site production | Manufacturing double-curved panels with conformal voids | Additive manfacturing: Material Extrusion | Use of a second temporary support material | Loughborough University | UK |
| 3 | Wet mix, cement mortar <10 mm | On-site and in-situ | The 'BOD': a 49m2 office building | Additive manfacturing: Material Extrusion | None | COBOD | Denmark |
| 4 | Wet mix, Cement mortar <4 mm | Off-site production | Shotcrete printing a reinforced double-curved concrete wall | Additive manfacturing: Particle-bed binding | Accelerating the setting, placement of reinforcement | TU Braunschweig | Germany |
| 5 | Cement paste bound sand <1 mm | Off-site production | Enabling weight reduction a 12 m footbridge | Additive manfacturing: Particle-bed binding | None | Dshape | Spain |
| 6 | Cement mortar <4 mm | Off-site production | Column and beam manufacture | Formative: Deforming | Accelerating the setting, placement of reinforcement | Ethz | Switzerland |
| 7 | Self compacting concrete <8 mm | Off-site production | Commerical panel manufacture using flexible moulds | Formative: Either Deforming, or Solidifaction | Casting, or material jetting | TU Delft | Netherlands |

(continued)

**Table 2.1** (continued)

| Case Study | Material | Application | Product | Process (Classification) | Sub-processes | Organisation | Country |
|---|---|---|---|---|---|---|---|
| 8 | Conventional concrete <20 mm | On-site and in-situ | Full scale, reinforced concrete wall production in-situ | Additive manfacturing: Material Extrusion | Vibrating nozzle and placement of reinforcement | huaShang Tenda | China |

### 2.4.1 *Printing and Assembling a 6.5 m Bicycle Bridge*

This case study describes the manufacture of the bicycle bridge installed in Gemert in the Netherlands in 2017, pictured in Fig. 2.2. It was made at Eindhoven University of Technology with an additive manufacturing process based on material extrusion (Salet et al. 2018).

**Process & facility details**

The material was supplied via a continuous mixing and pumping process. The position of print head is controlled via a g-code operated, large scale gantry robot with four degrees of freedom: the fourth degree required to keep the rectangular nozzle perpendicular to the direction of movement. A rectangular extrusion nozzle is used, programmed to remain tangential to the print path, Fig. 2.3 (Bos et al. 2016). The deposition quantity is adjustable, with a default setting of approximately 2.4 l/min. The print head can optionally be equipped with a cable reinforcement device capable of simultaneously applying flexible reinforcement cables into the print filament (Bos et al. 2017).

**Material details**

The material used was Weber 3D 115–1, a single-phase, shape stable, thixotropic, cementitious print mortar, comprised of CEM I Portland cement, aggregate (1 mm maximum particle size), filler and additives, rheology modifiers and a small amount of PP-fibres (Wolfs et al. 2018a, c). Although some experiments were performed, studies on hardened properties of Weber 3D 115–1 have not been published because

**Fig. 2.2** Completed bridge at the opening. *Phote* Kuppens fotografie


**Fig. 2.3** Printing of a bicycle bridge element

an improved version of the mortar was developed, Weber 3D 145–2, where details are given in (Wolfs et al. 2019b).

### Application details

The bridge consists of six identical horizontally printed elements that were rotated 90° after production, adhesively bonded with epoxy and prestressed with unbonded post-tensioned tendons, Fig. 2.4. The tendons are anchored in conventional cast concrete blocks at both ends of the bridge. Full prestress is applied, i.e. the full concrete section of the bridge remains in compression at all times. In each element, approximately the bottom 10% of layers are provided with a high strength steel reinforcement cable, entrained with the cable reinforcement device. The cable acts

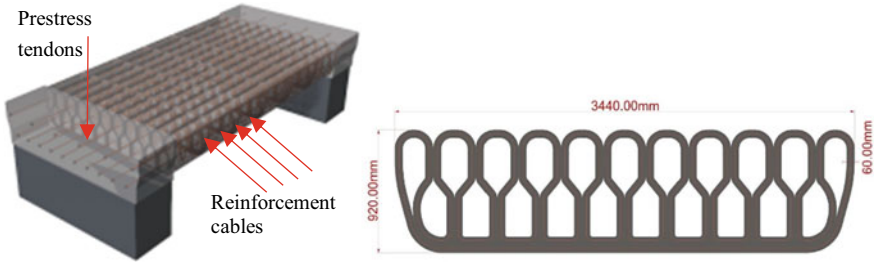


**Fig. 2.4** Schematic 3D image showing prestress tendons and reinforcement cable zones (left) and print element section geometry (right)


**Fig. 2.5** In-situ testing of the bridge with water-filled containers

as passive reinforcement in the transverse direction, while the prestress tendons provide active reinforcement in the longitudinal direction of the bridge. Figure 2.5 depicts the bridge under test in-situ (Bos et al. 2018).

The uniformly distributed design load was $q_{Ed} = 5.0$ kN/m$^2$. Prior to the project, the available data on the structural properties of the available print material (Weber 3D 115–1 mortar) was limited. Furthermore, the use of printed concrete or mortar was not covered by the structural engineering codes prevailing in the Netherlands. Therefore, extensive attention was paid to the structural safety, by adopting a 'fail-safe' design, i.e. a design that relied on a tried-and-true principle of a print concrete section entirely in compression (full prestress scenario), rather than on more uncertain properties such as tensile strength or the performance of innovative reinforcement technologies. The design was analysed through a full 3D Finite Element Analysis, to ensure that no unexpected local stress situations would cause structural damage. In addition, construction approval was obtained by applying the 'Design by Testing' option available in Annex D of the EN (1990). In addition to extensive material testing, there was also a 1:2 scale destructive mock-up test, Fig. 2.6, as well as an in-situ test to the serviceability limit state load, Fig. 2.5.

The print path followed the outer contour of the bridge and a bottle-shaped inner pattern, coming to 25.1 m length per layer (Fig. 2.4). Each element took approximately eight hours to print. The open internal structure allows room for the prestressing tendons.

As the prestress in the tendons results from their (forced) elongation, its level is directly dependent on any shortening of the concrete, which may be due to elastic deformations, creep and shrinkage. As printing mortars generally contain a relatively high cement content, they are more sensitive to these phenomena than ordinary concretes. Besides creep and shrinkage tests that have been performed preceding the


**Fig. 2.6** Scale model in 4-point bending test set-up

project, the bridge is therefore subjected to a long-term monitoring program, and the prestress system has been designed to allow future restressing.

### *2.4.2 Manufacturing Double-Curved Panels with Conformal Voids*

This case study describes the manufacture of double-curved panels with conformal voids manufactured as concept parts at Loughborough University in 2011, pictured in Fig. 2.7. The panels were made using an additive manufacturing process based on material extrusion in combination with a printed secondary support material (Lim et al. 2016).

**Process & facility details**

The extrusion-based printing process used a batch mixing approach supplying the cementitious mortar to storage and feed hopper and pumping process combined with a second extrusion head for printing the support material (Austin et al. 2011). Both printing heads were adjacently mounted in parallel on a large-scale gantry with three degrees of freedom, controlled through g-code. The materials were extruded through circular, 9 mm diameter, nozzles with a layer height of 6 mm less than the diameter, such that the top layer was flattened during printing, Fig. 2.8. The nozzle velocity was in the order of 30 mm/s (Lim et al. 2012).

**Fig. 2.7** Double-curved panels printed with conformal voids

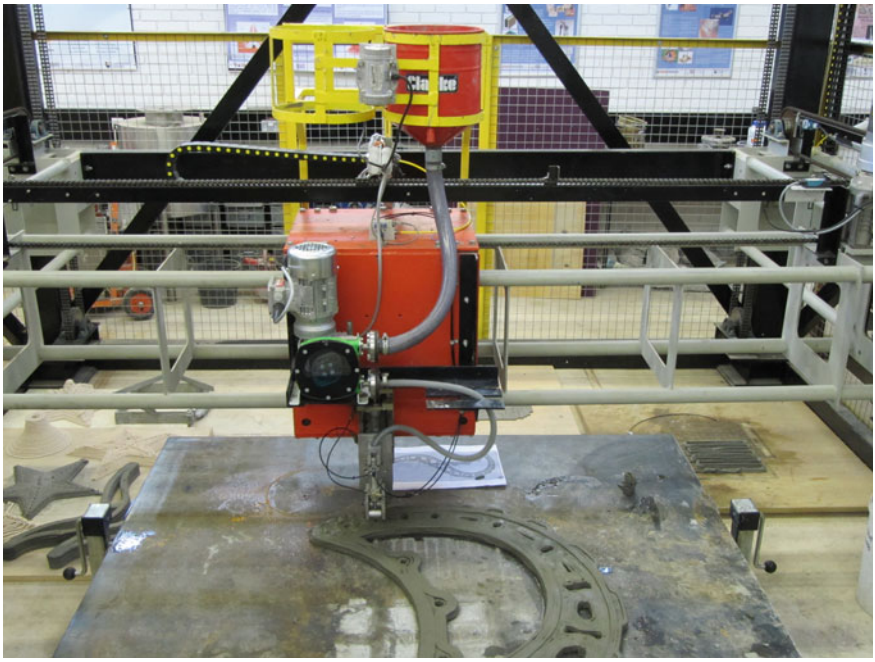

**Fig. 2.8** The mortar extrusion hopper and pump mounted on the gantry system

## Material details

The build material was a shape stable, thixotropic, cementitious print mortar, which comprised of CEM I Portland cement, fly ash and undensified silica fume, aggregate (2 mm maximum particle size), superplasticiser, retarder and some polypropylene microfibres (hardened properties: Le et al. 2012a and fresh properties: Le et al.

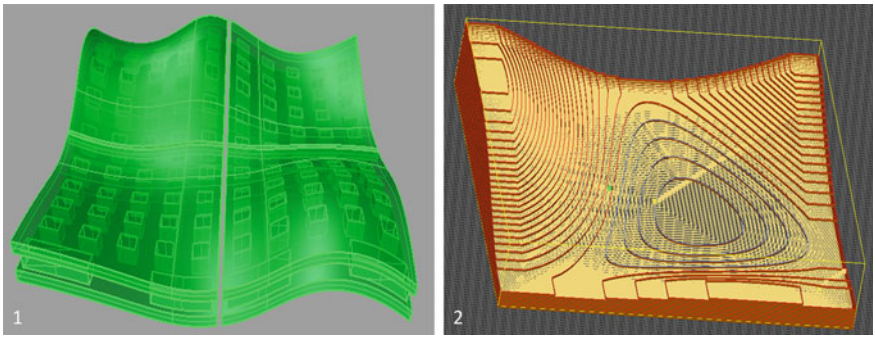


**Fig. 2.9** The 3D CAD model of the panels on the left and the right-hand image is of the model of the base component of sand support for the top right panel

2012b). The support material comprised of sand and a water-soluble binding agent that can be added in variable quantities to stiffen the printed material so that it could support the load of the wet build material.

### Application details

The four panels demonstrated the manufacture of the first fully three-dimensional geometry to be printed in mortar with conformal voids with the aid of a removable, temporary support material. The demonstrator comprised of four unique panels approximately 800 × 800 mm that formed a single, double-curved surface once assembled on a mounting frame (Fig. 2.7).

Similarly to conventional Additive Manufacturing processes, the generation of the machine instructions is derived from a 3D CAD model shown on the left-hand side of Fig. 2.9. Printing in flat layers for (relatively) thin curved panels can be cumbersome to achieve in practice and so a non-conventional approach was used. Tool paths that printed conformally to the surface were developed using Grasshopper and proved effective at improving efficiency, performance and surface quality (Lim et al. 2016).

The processing of the CAD model is more complicated with the support material: two models are required, one to base the generation of the tool path of the build material (cement-based mortar) (Fig. 2.9–1) and one for the creation of the support structure (Fig. 2.9–2).

Figure 2.10 depicts six stages of manufacture. Figure 2.10–1, shows the printing of the sand support to create the bottom curved working surface. Once the support was completed, the layers of the bottom shell are printed conformally on the base using the extruded mortar (Fig. 2.10–1). The internal voids and interconnecting ‘pillars’ are then formed, ensuring a good bond between the shell and pillar (Fig. 2.10–3).

The base support material of each part was relatively easy to define in CAD and was actually printed using a conventional flat layer approach, making the generation of the tool paths straightforward. As previously mentioned, generating conformal printing paths was more demanding and some considerable time invested in developing a Grasshopper tool to do this (Lim et al. 2016).


**Fig. 2.10** Six stages of manufacturing one of the panels and the CAD model compared to the finished parts

The support was dispensed via a specially designed tool that allowed the sand to be 'extruded' with very similar dimensions to the mortar, hence making the creation of the tool paths in the centre of the component (layers that were 50% solid and 50% void) easier to compute. However, the actual manufacture was challenging in practice and required some intervention to ensure the build was completed correctly.

Once the pillars and supporting material were in place, the top shell was printed, and the part left to cure, before being separated from the support and washed clean (Fig. 2.10–4, 5 and 6). Figure 2.10–7 and 8 depict the CAD model and the finished component.

The CAD model for each panel was extracted from the whole surface and was printed over-sized by 25–50 mm so that the precise joints between each panel can be located and cut using a conventional diamond saw. This was done by hand in this test application, but it could be automated.

The addition of the second support material enables far more freedom in the components that can be designed and manufactured, although this needs to be

traded off in the greater processing burden and the more complex interaction of two deposition systems.

### 2.4.3 The 'BOD': A 49 $m^2$ Office Building

This case study describes an extrusion-based additive approach that utilises a mix design containing recycled aggregates to print the walls of a building in-situ rather than in the factory (as the approaches from Sects. 3.1 and 3.2). The project was completed by COBOD International (former 3DPrintHuset) in Nordhavn, Denmark in 2017, Fig. 2.11–8.

**Process & facility details**

The extrusion-based print process was carried out in-situ using batch mixing and a continuous pumping system to deliver material to a hopper mounted on a large gantry system having four degrees of freedom. A rectangular extrusion nozzle (50 × 10 mm) was used for most of the construction, and the nozzle orientation is set to remain tangential to the print path. The average volume flow rate for the extrusion was 0.36 $m^3$/h, although this was adjusted several times during the process. The maximum travel velocity of the printing head reached 100 mm/s, while the practical travel speed was found to be about 60% of this.

**Material details**

A custom-design concrete mix based on CEM II was used. This mix included fine aggregates with a maximum particle size of 4.0 mm. In addition, crushed-red roofing tiles and bricks were used. The fine and recycled aggregates were pre-mixed prior to delivery. Immediately before printing, the pre-mixed aggregates were placed into a concrete mixer (100 L drum mixer) in which cement, water, polypropylene fibres and superplasticizer were added. The pre-mixed material was then transported to a progressive cavity pump, which conveyed the material to an extrusion nozzle (Fig. 2.11–3) that works under a screw system principle. The mix design is listed in Table 2.2 and yielded a compressive strength of 52.0 MPa.

It is worth mentioning that during the initial phase of the printing process, it was observed that the pre-mixed aggregates (especially the recycled fraction) were out of specification in relation to the maximum particle size, which was problematic for pumping. It turned out that more than 10% of the aggregates were above not only 4 mm but up to 20 mm. This resulted in clogging the hose when pumping and the subsequent pressure build-up ruptured the supply hose in one printing sessions. Subsequently, the premixed materials were sieved using a 10 mm sieve. Hence, the final mix comprised aggregate particles with size up to 10 mm.

**Application details**

The project was the first 3DCP building project to receive an approval/permit by a municipality in Europe. The printing process was intended to be applied to the


**Fig. 2.11** Main phases in the construction of the BOD: 1. 3DCP of the foundation slab contour; 2. Concrete casting of the foundation slab; 3. 3DCP of the building walls and printing nozzle; 4. Detail of the insulation material; 5. Detail of the manually added rebars; 6. The BOD walls right after printing; 7. Application of roof, doors and windows; 8. The BOD after its completion

**Table 2.2** Mix design of the concrete used in 'The BOD'

| Materials | Composition [kg/m$^3$] | Mass Fraction [kg/kg] | Total mass [ton] | Total Cost [Euro] |
|---|---|---|---|---|
| CEM II | 735.4 | 1.00 | 6.12 | 1,392 |
| Sand N.1: 0–2 mm | 420.6 | 0.57 | 3.50 | 79 |
| Sand N.2: 0–4 mm | 420.6 | 0.57 | 3.50 | 86 |
| Recycled agg.: 0–4 mm[a] | 526.3 | 0.72 | 4.38 | 70 |
| Superplasticizer | 4.8 | 0.007 | 0.04 | 26 |
| Polypropylene fibres | 2.4 | 0.003 | 0.02 | 139 |
| Water | 199.5 | 0.27 | 1.66 | 8 |
| **Total** | – | – | 19.22 | 1,800 |

[a]Specification provided by the producer, thought the maximum particle size was up to 10 mm

building of the walls and structural columns that carry the roof. However, the subcontractor in charge of executing the foundation slab faced challenges to produce a formwork that matched the shape of the building and, hence, 3DCP was also used to print the external perimeter of the foundation (total height of 600 mm, Fig. 2.11–1). Traditional casting method was then used to form the foundation (Fig. 2.11–2).

This allowed for the placement of reinforcement using standard practices; thus, the structural elements were produced to existing codes—leaving the printed parts as a permanent formwork. The installation of the roof, windows, doors and surface finishes was carried out using standard building practices. Similar to the foundation, the printed walls (Fig. 2.11–3 to 5) were not considered as load-bearing elements. For the load-bearing elements such as columns, a similar formwork approach was applied to produce 11 columns that were also reinforced and then cast to carry the imposed loads.

The 3DCP of the foundation perimeter, walls and columns were finalised in about two months; six weeks of which were spent adjusting the process to cope with the problems with the pre-mixed materials. The project was complete in eight months, mainly due to the availability of labour. Without interruption, the total printing time was approximately 55 h.

### *2.4.4 Shotcrete Printing a Reinforced Double-Curved Concrete Wall*

In this study, the manufacture of a double-curved wall is carried out (Fig. 2.12–6) with an additive manufacturing process based on material jetting (Neudecker et al.


**Fig. 2.12** Fabrication process; 1. Shotcrete 3D Printing of the wall; 2. manual placement of the pre-bent horizontal reinforcement; 3. precise cutting of the surface, while the concrete is still in the plastic state; 4. threading in the vertical reinforcement; 5. embedding the reinforcement by vertically spraying onto the printed structure; 6. final trowelling with a rotating plastic disc

2016), as opposed to material extrusion, discussed in Sects. 3.1, 3.2 and 3.3. The incorporation of reinforcement is demonstrated using a dual application approach and was realised at Technical University of Braunschweig.

**Material details**

In shotcrete 3D Printing (SC3DP), the layers are built up by a spray deposition (or jetting) process using compressed air to carry the materials to the working plane. It is an evolution of the traditional shotcrete processes. The jetting velocity results in very good bonding behaviour between layers (Nolte et al. 2018) and the ability to encase reinforcement. A pre-mixed cement-based mortar is mixed in a conventional batch mixing approach and is subsequently conveyed to the printing nozzle using standard pumping equipment. An accelerator is added at the nozzle to enable faster building rates.

**Process details**

The print head is mounted on a large gantry system with two vertical axes of which one is equipped with a six-axes robot and the other with a three-axes milling device. The overall cooperative build volume is 10.5 × 5.25 × 2.5 m high.

The nozzle velocity was set to 0.25 m/s, resulting in a layer height of 1 cm. This enables a material deposition rate of $1m^3$ per hour. For this specific case-study, the total printing path length was added up to be 675 m, resulting in a (calculated) printing time of 45 min. After every 40 layers, the printing process was paused, and pre-fabricated 10 mm horizontal steel reinforcement elements were manually placed lengthening the actual manufacturing time to 80 min.

**Application details**

To demonstrate both the structural and design potential of shotcrete printing, a concept part was designed: a double-curved, reinforced concrete wall with high surface quality. The wall has a length of 2.5 m, a thickness of 18 cm and a height of 2.3 m. The manufacture of the wall integrated the shaping and the placement of structural reinforcement. In addition, the surface finish of the sprayed component has a rather coarse resolution and so to address this, subtractive processing for surfaces and edges were applied.

The modelling process included a structural analysis of the geometry using, Rhino 3D (www.rhino3d.com) and Karamba (www.karamba3d.com) for Grasshopper (www.grasshopper3d.com) to test that the wall would be stable during manufacture. The wall was realised using two spraying processes. The first spraying operation used flat layers in an additive manufacture fashion to form the core of the wall (Fig. 2.12–1), pausing to hand place pre-bent horizontal reinforcement (Fig. 2.12–2). While the concrete was still plastic, a subtractive process was applied to improve the potential jointing surfaces (Fig. 2.12–3). Vertical reinforcement was then added (Fig. 2.12–4), utilising the undulating profile of the core print. The reinforcement was encapsulated with the second sprayed layer application in the vertical direction (Fig. 2.12–5) and then trowelled smooth, again while the concrete was plastic (Fig. 2.12–6).

Currently, the fabrication process requires a team of at least five people. Three people are needed for handling the concrete supply chain, one to control the machine and one to supervise the process and to intervene should problems arise.

### *2.4.5 Enabling Weight Reduction of a 12 m Footbridge*

This case study describes a 12 m long footbridge, installed in Madrid, Spain by Acciona in 2017 (Fig. 2.13). The D-Shape® process was used to realise weight reduction in an assembly of eight pieces that form the bridge. This additive manufacturing process uses a particle-bed and binder approach, rather than the

**Fig. 2.13** The footpath bridge in Madrid by Acciona (© Enrico Dini)

deposition of a pre-mixed wet mortar used in extrusion and jetting methods mentioned in previous case studies (Valencia 2017).

**Material Details**

The material is a compacted, dry sand (maximum particle size of 0.2 mm) spread and cement that is locally activated by spraying or jetting water or a water-admixture solution into the packed particles thus forming a cement paste matrix around the aggregate particles. Capillary effects draw the water into the matrix, and the water spreads out to the size of the nominal voxel. Careful compaction of the matrix material is critical to control the dispersion of water in the voxel and ensure that full layer penetration is achieved as these factors affect the resultant mechanical properties (Lowke et al. 2018).

**Process Details**

In general, the printing process consists of two repetitive work steps. In the first step, a layer of dry particles is spread over the printing area with a uniform thickness of about 5 to 10 mm. The second step is the selective deposition of a fluid onto the particle bed by means of a print head in order to bind the particles. This process is repeated in series until the component is complete. Once cured, the non-bonded particles are removed in a post-processing step of de-powdering, Fig. 2.14 (Lowke et al. 2018).

There are two methods of binding the particles: either by selective paste intrusion, where a cement paste is deposited on the surface to the packed bed and is drawn into the dry material under gravity (Pierre et al. 2018), or where the cement component is added in its dry state to the particle-bed, before it is selectively activated by adding water to the surface. In this case study, the footbridge was manufactured using selective cement activation.

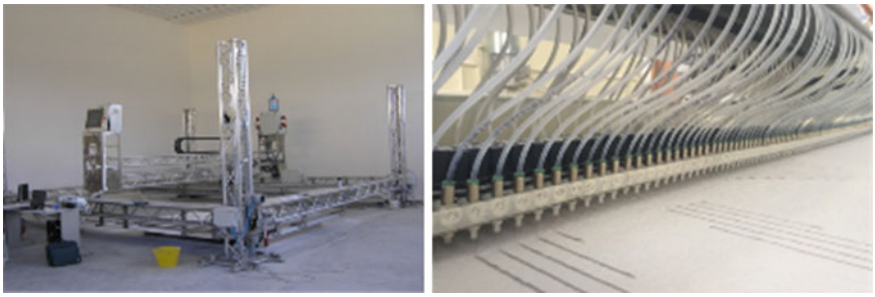

**Fig. 2.14** D Shape® 3D-printer (left) and print head (right) (Lowke et al. 2018)

The D Shape® printer used in manufacture consists of a horizontal aluminium frame lifted by four columns giving a print area of $2 \times 2 \times 2$ m$^3$. The horizontal frame contains a print head with 100 nozzles at 20 mm intervals and a blade to spread the sand. To fill the gaps within the array of nozzles and to ensure that the whole cross-section would be uniformly reached by the fluid, each layer is produced in multiple passes with a 5 mm offset of the print head, Fig. 2.14. The average printing speed of the printhead is around 15–20 cm/sec.

**Application details**

A D Shape® particle-bed binding printer was used to build a footpath bridge shown in Fig. 2.13. The bridge has a total length of 12 m, a width of 1.5 m and a bridge railing height of 1.3 m (IAAC 2019). The supporting structure of the bridge consists of two lateral Vierendeel metal structures and eight printed concrete elements. The metal structure has a variable height of about 1.3 m at the supports and 1.1 m in the middle of the bridge. The forces introduced into the structure are transmitted through the metal structure to the supports located on the two banks. During the building process, the metal structures were installed first followed by the modular installation of the printed concrete elements. Figure 2.15 gives a schematic overview of the installation process.

### *2.4.6 Column and Beam Manufacture*

Here, Smart Dynamic Casting is applied to manufacture the façade mullions installed in the DFAB house at the NEST building on the Empa campus in Düben-dorf, Switzerland (Fig. 2.16). The process is based on the principles of slip-forming and is a formative process that deploys extrusion vertically to shape the cross-sectional area of beams and columns. The cross-sectional area can be either rigid, or adjusted to provide customisation (Lloret et al. 2019).

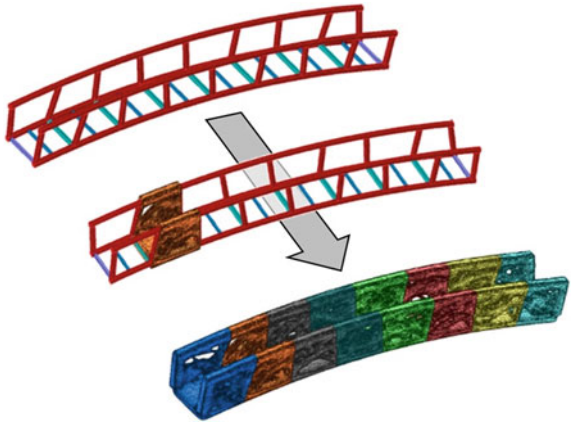

**Fig. 2.15** Substructure and building process of the footpath bridge (Acciona 2019)

**Fig. 2.16** Final installation of façade mullions in the DFAB House, on the left-hand side of the image

### Material details

The approach used a cement mortar with a maximum aggregate size of 4 mm, which is batch mixed conventionally. The method relies on shaping concrete in the moments when it is still plastic but has adequate strength to support its own weight as well as the weight of some additional concrete within the formwork (Lloret et al. 2015, 2016). To achieve this, the measurement of the material to determine its plastic state, and the control of setting through the addition of admixtures just before deposition into the formwork are critical aspects to the process (Mettler et al. 2016; Lloret et al. 2017). Controlling when this moment occurs and timing it correctly with the vertical slipping speed, is crucial. Slipping too fast will cause plastic collapse of the material lacking enough strength. Too slow slipping will result in high friction within the formwork and brittle failure from a material that has almost set.

### Process details

SDC is a scaled-down version of slip-forming, or vertical extrusion, in which a vertically moving and reconfigurable formwork shapes gravity-fed material either within the formwork, or at the moment it exits. The material is a batch mixed, cement-based mortar which is then deposited into the formwork either manually or via a pump.

The formwork is about 40 cm in height, and 80–800 $cm^2$ in cross-sectional area depending on the specific implementation. It moves at a vertical slipping speed of 10–20 mm/min via either a 6-axis robotic arm or a linear axis. The columns can be deformed by rotation of the formwork on the robotic arm, or via a rotating table at the base of the linear axis (Fig. 2.17–1); by linear actuators placed at the bottom of the

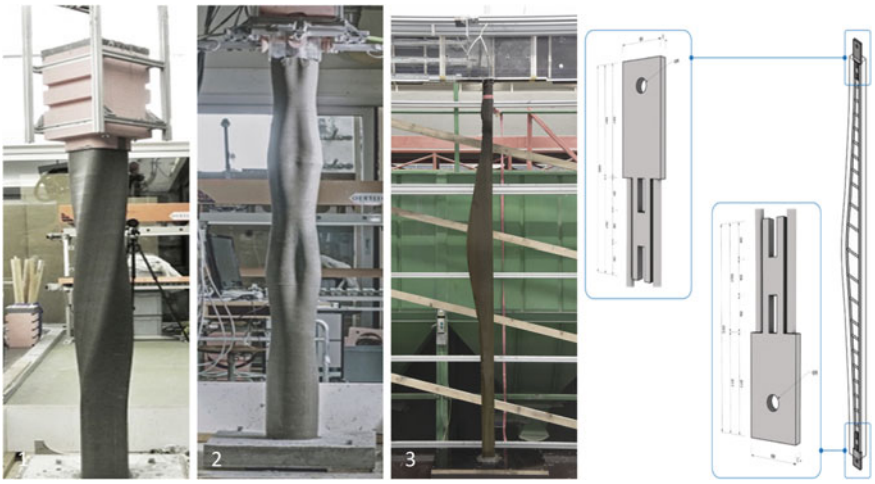


**Fig. 2.17** 1. rigid formwork, rotational deformation; 2. rigid formwork, linear actuator deformation at exit; 3. single sided deformation, reinforced column demonstrator; 4. schematic of top and bottom couplers used in tensioning reinforcement for production

**Fig. 2.18** Process details for application 3 in Fig. 2.17: 1. linear actuators for deformation within formwork; 2. scaled metallic strip for deformation; 3. capillary oiling system in constructed formwork

rigid formwork, requiring the placement of a void space in the centre of the column to allow the incompressible material a place to flow (Fig. 2.17–2); or by the use of linear actuators, on one or two sides, is moved vertically to change the rectangular in cross-sectional area (Fig. 2.17–3).

Formwork friction is minimised through the use of low-friction synthetic material inside the formwork as well as the installation of capillary oiling systems. In the latter application, a forming strip (Fig. 2.18–2) is coupled magnetically to the actuators (Fig. 2.18–1), and is 'scaled' to allow flexible deformation and entry of oil via a capillary oiling system (Fig. 2.18–3). Formwork friction was monitored with process feedback using load cells mounted on the formwork. Strength build-up was monitored by measuring formwork pressure at a sensor positioned just before material exit (Lloret et al. 2017, 2019).

**Application details**

The reinforced façade mullions in the DFAB house in Dübendorf, Switzerland, were manufactured using the flexible formwork approach depicted in Fig. 2.17–3. This method has been demonstrated to be more versatile than the fixed formwork methods depicted in Fig. 2.17–1 and 2.

In total 15 mullions were manufactured for the DFAB house, each with a different form to match required material amounts in the centre of the mullion with calculated façade wind loads and variable tributary lengths. The mullions were approximately 3 m high, and each took approximately 3 h to slip-form, and approximately 8 h in total production time per mullion.

During the manufacturing set-up, the reinforcement sections (Fig. 2.17–4) were cut, bent and welded prior to slip forming. Coupling plates were fitted to each end such that the reinforcement could be held vertically and tensioned during manufacture, and the same plates were used for on-site installation. For production, the mould system was then installed around the reinforcement, and the slip forming then carried out to completion of the mullion (Lloret et al. 2019).

One complicating factor for the application of these methods is the precision in the control of the curing required. In addition, the loss of the formwork leads to a

higher risk of drying shrinkage cracks and deformation. In the DFAB house, these issues are being treated by through life monitoring.

### *2.4.7 Commercial Panel Manufacture Using Flexible Moulds*

Flexible moulding is a DFC technology that has been used on various commercial projects including the Arnhem OV Hub in the Netherlands (architect UNStudio, concrete product manufacturer mbX), the interior cladding of two Crossrail underground stations in London (architect Grimshaw, panels by mbX) and Kuwait International Airport terminal vaulted roof (architect Foster + partners, panels by Limak / Adapa). The method can be deployed as a deformation process, where the panels are shaped after casting (used in the former two examples) or as a solidification process, where the moulds are deformed before material placement (in the latter example), Fig. 2.19.

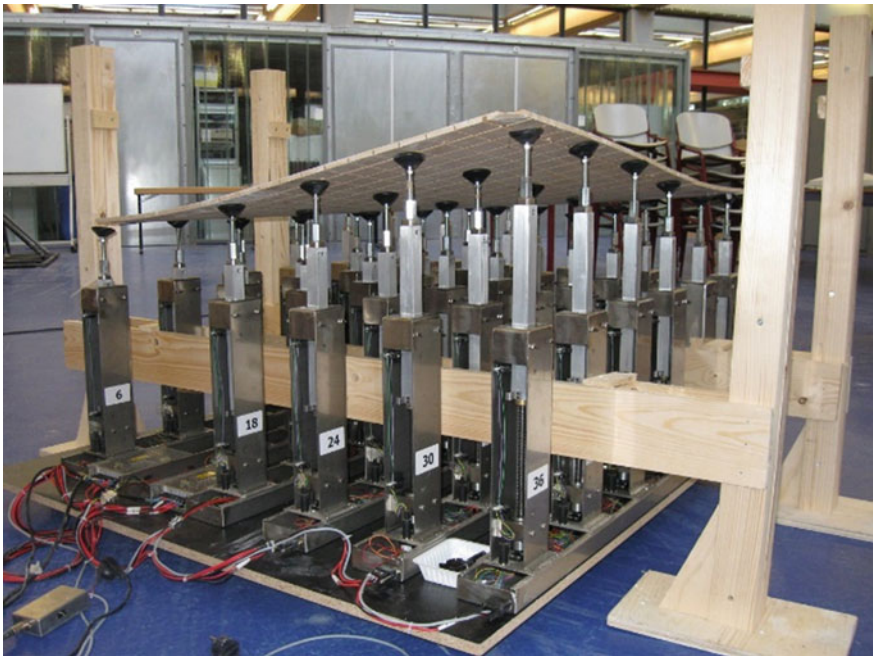


**Fig. 2.19** Prototype mould of Vollers and Rietbergen at TU Delft (2010) (patent described in Vollers et al. 2010)

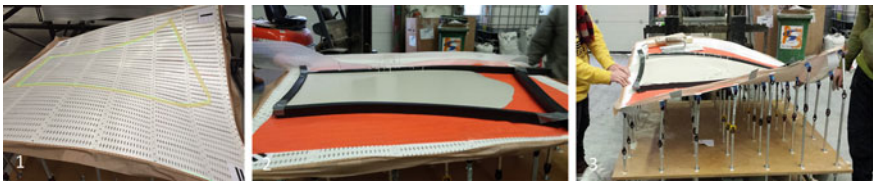

**Fig. 2.20** Prototype of the flexible mould as developed in a Dutch R&D project operating in mode 1, deformation: Setting out formwork (Schipper et al. 2015b)

**Fig. 2.21** Images from the realisation of Kuwait International Airport using flexible moulds from Adapa: 1. artists impression of the finished building; 2. the pin bead and mould surface; 3. and 6. an on-site mock-up of the panels; 4. and 5. production facilities required for the industrial-scale manufacture of the roof

### Material details

Typically, self-compacting concretes or zero-slump concretes for spray applications are used, depending on system configuration, see Table 2.3. In mode 1 (deformation), the control of the thixotropy is critical. A fast, initial setting of the fluid concrete is needed, to allow for deformation without spilling. At the same time, the material should still be sufficiently plastic/compliant to prevent cracking during this deformation (Schipper et al. 2015a).

In mode 2 (solidification), once the mould is deformed first, the concrete is applied on a sloping mould surface, requiring that the yield strength of the mixture is high enough to resist gravity. Often spraying is used. If a zero-slump concrete is applied, the process is comparable to plastering or rendering.

Mode 1 only allows for compliant reinforcement, such as very thin steel nets, short or long chopped fibres in steel, PVA or glass, or alkali-resistant textiles in glass-fibre. Mode 2, due to the application method of the concrete, is mostly served

**Fig. 2.22** The completed two-story villa

**Table 2.3** Typical concrete mix for a self-compacting HPC with an average cube compressive strength (28 days, cubes with 150 mm ribs) of 76 MPa and an average prism flexural strength (28 days, prisms 40 × 40 × 160 $mm^3$) of 13 MPa

| Concrete component | KG/1000 L |
|---|---|
| Cement CEM I 52.% R white | 600 |
| White limestone powder (Betoflow D, O) | 180 |
| White pigment | 6 |
| PVA Fibers L = 8 mm (Kuraray) | 5.2 |
| Superplasticizer Glenium 51 (BASF) | 3.2 |
| Water | 228 |
| Sand 0.125–0.25 mm | 229 |
| Sand 0.125–0.25 mm | 408 |
| Sand 0.5–1 mm | 637 |

by short fibres that can be mixed and sprayed together with the concrete, but can also be applied in combination with regular steel reinforcement, like in the Kuwait airport case.

### Process details

The process is based on reconfigurable pin bed is deployed in one of two ways: either as part of a deformation process, where the material is cast flat and the

pin bed deformed while the material is compliant (mode 1, Fig. 2.20); or as a solidification process where the mould shape is determined prior to the addition of the material (mode 2). The method is typically used for creating non-structural panels of 10 to 50 mm thickness used for non-structural applications, such as façade or roof cladding in free-form architecture that has limited repetition of standard elements. It is also used to produce panels that are used in structural applications as permanent formwork of volumetric curved concrete structures (e.g. curved bridge decks or curved structural concrete roofs of which the thin shell is topped with in-situ traditionally reinforced concrete).

The flexible mould consists of an elastic, rubber-like surface containing steel rods in two directions to guide and smoothen the deformation of the rubber mat (Fig. 2.20–2). On this rubber mat, it is possible to cast or deposit any mouldable and solidifying material. The shape of the rubber mat can be controlled with CNC-controlled actuators directly from the 3D-file from flat into any doubly curved surface (Fig. 2.20–3). The contours of the elements are placed manually on the surface after conventional laser projection on the exact location (Fig. 2.20–1), which is non-trivial in a doubly-curved geometry (Schipper and Eigenraam 2016).

**Application details**

Among the first companies to really deploy the adaptive mould at full industrial scale and within a digitally driven process is Adapa, holding various patents in the field (Kristensen and Raun 201; Raun and Henriksen 2014). At the time of writing (2019–2020), Adapa is involved in the construction of Kuwait International Airport, an immense 1.2 km length terminal designed by Foster + Partners and ARUP, comprising vaulted, parametrically shaped roofs with very limited repetition of panels.

The sheer size, number of panels, and lack of repetition forced the designers to prescribe the use of a digitally controlled flexible mould in the brief, to make the project feasible. Figure 2.21–1 shows an artist impression of one of the terminal areas. The smooth rubber surface and the digitally controlled actuators of an Adapa mould are visible in 2.21–2. For the Kuwait project, a steel edge profile was used as a delimiter for the concrete, whereas the adaptable mould surface forms the basis of each cast, each panel having a slightly different curvature. Traditional reinforcement is placed before casting. Figure 2.21–5 gives an impression of the production line needed for this immense project. Fugure 2.21–3 and 6 are on-site mock-ups of the produced vault and cladding panels.

An advantage of the process is the architectural surface quality of the parts; however, as concrete is alkaline, it shortens the life of the rubber used as the flexible casting surface.

### 2.4.8 *In-Situ Production of Full Scale, Reinforced Concrete Walls*

This final case study presents the production of a residential villa, in Tongzhou, Beijing, China in 2016 by HuaShang Tenda, Fig. 2.22. The case study illustrates construction automation enabled by material extrusion using conventional concrete in such a way as to encase preplaced reinforcement mesh.

**Material details**

The material used is ordinary vibrated concrete comprised of Portland cement, sand (0–5 mm), coarse aggregates (5–20 mm) and water. No additives were used. The average compressive strength of hardened concrete was between 30 and 40 MPa. Concrete is produced in a conventional gravity mixer with a capacity of 1 $m^3$ and placed batch by batch into the hopper. When filled, the printhead can accommodate approximately 0.3 $m^3$ concrete.

**Process details**

The material is conveyed vertically in the large printhead under gravity, assisted by vibration. The vibration is generated by an unbalanced mass and propagates along the length of the nozzle. The nozzle is forked and held by the print head mounted on a large-scale gantry robot with four degrees of freedom, including rotation (Fig. 2.23–1).

The outer dimensions of the application reported here are 15 × 15 × 9 m. The gantry system carrying the printhead is 20 m wide and moves on rails (Fig. 2.23–1). The vertical steel mesh reinforcement is fixed by hand prior to printing. The concrete is then deposited layer-by-layer, gradually enclosing the reinforcing bars from all sides, see Fig. 2.23–3 and –1 to 3.

A given machine configuration is designed to operate at a constant volume flow rate, and the velocity of the printhead horizontal movement during the construction of the villa was approximately 0.3 m/min while printing the 100 mm thick walls. The average thickness of each layer was 50 mm.

**Application details**

This project realised a two-storey, 400 $m^2$ villa on the grounds of the company in Tongzhou Beijing, China. The design was performed according to the Chinese code (incl. earthquake load case). The layout planning was carried out with AutoCAD. The foundation slab with connective reinforcement was produced in a conventional manner, see Fig. 2.23–3. The vertical steel mesh reinforcement and plastic installation tubes were placed manually. The vertical walls, both straight and curved, were then manufactured additively by deposition of concrete layers which encapsulated the reinforcement and tubes. At openings (doors, windows) the concrete conveying was interrupted, and some manual help was provided to ensure the desired geometrical accuracy. Provisory wooden supports were sutilised to deposit concrete over the openings. The ceilings and the roof were made of composite slabs (manually placed

profiled steel sheets served as permanent formwork and concrete was deposited automatically upon them).

Although the vibration is applied at a considerable distance from the nozzle orifices, they propagate towards the orifices, resulting in quasi-compaction of concrete, improving the quality of both concrete and bond between concrete and reinforcement. It should be noted that reinforcement mats provide kind of stabilising support to the freshly deposited concrete layers; however, the extent of such effect still needs to be investigated.

The concrete works were carried out between mid of October and end of November 2015 on the firm's compound using the printer built the same year. The entire building process took 45 days, according to HuaShang Tengda Ltd.

The approach is promising; however, at this stage, it exhibits some limitations. First, the height of individual mesh sheets is limited to the size of the forked nozzle, which is quite large: here the mesh sheet height was approximately 1.7 m while the height of the entire printhead was approximately 3.5 m. The second limitation is that only one or two reinforcement layers can be easily integrated into the middle of the wall cross-section. However, not only reinforcement but also some simple installations such as cable tubes and even thermal insulation can be accommodated, see Fig. 2.23–4. Furthermore, only vertical walls (no inclination) and only rounded transitions (no sharp corners) can be produced, while the walls' surfaces exhibit a rough texture, see Fig. 2.24. Finally, since the gantry system must be very massive


**Fig. 2.23** On-site 3D-printing by HuaShang Tengda: 1. gantry-based printer with a hopper on the top of the printhead; 2. raw materials and mixer; 3. foundation and connective steel bars; 4. deposition of the first layer


**Fig. 2.24** Construction of the two-storey villa: 1. forked nozzle lays concrete on both sides of the rebars, 2. printing a bow; 3. manual help at the opening, when the material flow is interrupted; 4. forming a vertical element

and stiff to enable a robust control of a heavy and vibrating printhead, the transport and mounting of such printer limit its mobility and flexibility.

## 2.5 Summary and Outlook

This chapter provided a brief background of contemporary DFC and demonstrated the diversity in existing technologies. These differences are more than skin deep and are often driven by the product that the process is designed (or optimised) to produce. In one case study (Sect. 3.7), the actual implementation of the technology determined its classification.

By acknowledging the type of *Material* used, the *Application* environment, the *Product* and the *Process* it is possible to clearly delimit the scope of a technology and so identify differences and similarities that would otherwise not be obvious. The MAPP definitions should also identify the enabling sub-processes that are necessary during fabrication as these are often where important differences are found. Nonetheless, the method classification should be based on the main assembly, or material forming process, following convention.

Eight representative case studies which fit within the classification framework were used to illustrate the similarities and the differences between materials, applications, products and processes, Summarised in Table 2.1. The process descriptions have never been brought together in this way before, and we hope that readers find the case studies informative in their own right, but also a useful resource on which to reflect when understanding how to more appropriately compare and contrast difference DFC technologies.

**Acknowledgements** The work was supported by: the UK Industrial Strategy Challenge Fund: Transforming Construction initiative (EPSRC grant number EP/S031405/1) and EPSRC Grant number EP/P031420/1; the I-Site Future initiative, through the DiXite program at Gustave Eiffel University, Paris, France; the Swiss National Science Foundation, National Centre for Competence in Research: Digital Fabrication in Architecture; the Deutsche Forschungsgemeinschaft (DFG, German Research Foundation), Project Number 387152958 (GZ: ME 2938/20-1), within the priority program SPP 2005 OPUS FLUIDUM FUTURUM – Rheology of reactive, multiscale, multiphase construction materials; the Innovation Fund Denmark (Grant no. 8055-00030B: Next Generation of 3D-printed Concrete Structures); the Junior Professorship for Digital Building Fabrication is sponsored by the Gerhard and Karin Matthäi Foundation; the development of the Shotcrete 3D Printing technology (SC3DP) was funded by the Ministry for Science and Culture (MWK) of Lower Saxony and implemented with the DFG-funded Digital Building Fabrication Laboratory (DBFL). Mr. Wu from HuaShang Tenda provided information on the construction of the residential villa in Tongzhou, Beijing as well as Figs. 2.23-3 and 4 and 2.24.

## References

Acciona. (2019). 3D Printing Skill Center. Personal communication, November 28th, 2019.

Andersen, T. J., Leal da Silva, W. R. , and Thrane, L. N. (2016). Lessons from the TailorCrete Project. Concrete International, 38(3), 54–61.

Asprone, D., Menna, C., Bos, F.P., Salet, T.A.M., Mata-Falcón, J., and Kaufmann, W. (2018). Rethinking reinforcement for digital fabrication with concrete. Cement and Concrete Research, 112(S.I.), 111–121. DOI: https://doi.org/10.1016/j.cemconres.2018.05.020.

Austin S., Buswell, R. A., Lim, S., and Webster, J. (2011). *EP2886277A1*. Method and apparatus for delivery of cementitious material [PDF file]. Retrieved from: https://patents.google.com/patent/EP2886277A1/en.

Barbosa, F., Woetzel, J., Mischke, J., Ribeirinho, M. J., Sridhar, M., Parsons, M. Bertram, N., and Brown, S. (2017). Reinventing construction: a route to higher productivity [PDF file]. Retrieved from: https://www.mckinsey.com/~/media/McKinsey/Industries/Capital%20Projects%20and%20Infrastructure/Our%20Insights/Reinventing%20construction%20through%20a%20productivity%20revolution/MGI-Reinventing-Construction-Executive-summary.ashx.

Bonwetsch, T. (2015). Robotically assembled brickwork: Manipulating assembly processes of discrete elements. PhD Thesis, ETHZ. DOI: https://doi.org/10.3929/ethz-a-010602028.

Bos, F., Wolfs, R., Ahmed, Z., and Salet, T. (2016). Additive manufacturing of concrete in construction: potentials and challenges of 3D concrete printing. Virtual and Physical Prototyping, 11(3), 209–225. DOI: https://doi.org/10.1080/17452759.2016.1209867.

Bos, F., Ahmed, Z., Jutinov, E. R., and Salet, T. (2017). Experimental Exploration Metal Cable as Reinforcement in 3D Printed Concrete. Materials (Basel), 10(11), E1314. DOI: https://doi.org/10.3390/ma10111314.

Bos, F., Ahmed, Z., Wolfs, R., and Salet, T. (2018). 3D Printing Concrete with Reinforcement. In: D. A. Hordijk, M. Luković (Eds.), High Tech Concrete: where Technology Engineering Meet, Springer International Publishing, pp. 2484–2493. DOI: https://doi.org/10.1007/978-3-319-59471-2_283.

Buchli, J., Giftthaler, M., Kumar, N., Lussi, M., Sandy, T., Dörfler, K., and Hack, N. (2018). Digital in situ fabrication—Challenges and opportunities for robotic in situ fabrication in architecture, construction, and beyond. Cement and Concrete Research, 112(S.I.), 66–75. DOI: https://doi.org/10.1016/j.cemconres.2018.05.013.

Buswell, R. A., Leal da Silva, W. R., Jones, S. Z., and Dirrenberger, J. (2018). 3D printing using concrete extrusion: A roadmap for research. Cement and Concrete Research, 112(S.I.), 37–49. DOI: https://doi.org/10.1016/j.cemconres.2018.05.006.

Buswell, R. A., Leal da Silva, W. R., Bos, F. P., Schipper, R., Lowke, D., Hack, N., Kloft, H., Mechtcherine, V., Wangler, T., and Roussel, N. (2020). A process classification framework for defining and describing Digital Fabrication with Concrete. Cement and Concrete Research. 134(S.I.). DOI: https://doi.org/10.1016/j.cemconres.2020.106068.

Changali, S., Mohammad, A., and van Nieuwland, M. (2015). The construction productivity imperative. McKinsey Productivity Sciences Center [PDF file]. Retrieved from: https://www.mckinsey.com/~/media/McKinsey/Industries/Capital%20Projects%20and%20Infrastructure/Our%20Insights/The%20construction%20productivity%20imperative/The%20construction%20productivity%20imperative.ashx.

Egan, J. (1998). Rethinking Construction, Department of the Environment, London [PDF file]. Retrieved from: http://constructingexcellence.org.uk/wp-content/uploads/2014/10/rethinking_construction_report.pdf.

HMGov. (2017). Industrial strategy: building a Britain fit for the future [PDF file]. Retrived from: https://assets.publishing.service.gov.uk/government/uploads/system/uploads/attachment_data/file/664563/industrial-strategy-white-paper-web-ready-version.pdf.

EN 1990:2002 (2002), Eurocode 0—Basis of structural design.

Gambao, E., Balaguer, C., and Gebhart, F. (2000). Robot Assembley System for Computer-integrated Construction. Automation in Construction, 9(5-6), 479–487. DOI: https://doi.org/10.1016/S0926-5805(00)00059-5.

Gibson, D. Rosen, B., and Stucker. (2015). Additive Manufacturing Technologies: 3D Printing, Rapid Prototyping, and Direct Digital Manufacturing, Springer, New York, p. 498. DOI: https://doi.org/10.1007/978-1-4939-2113-3.

Garcia, M. (2010). AD+ Practice Profile: Amanda Levete Architects (AL_A). In Architectural Design, Published online 27th January 2010. Accessed 6/4/2020. DOI:https://doi.org/10.1002/ad.1019.

Gosselin, C., Duballet, R., Roux, P., Gaudillière, N., Dirrenberger, J., and Morel, P. (2016). Large-scale 3d printing of ultra-high performance concrete—a new processing route for architects and builders. Materials & Design, 100(-), 102–109. DOI: https://doi.org/10.1016/j.matdes.2016.03.097.

Groover, P. (2012). Introduction to manufacturing processes, John Wiley & Sons. p. 720. ISBN: 978–0470632284.

Hack, N., Lauer, W., Langenberg, S., Gramazio, F., and Kohler, M. (2013). Overcoming Repetition: Robotic Fabrication Processes at a Large Scale. International Journal of Architectural Computing, 11(3), 285–299. DOI: https://doi.org/10.1260/1478-0771.11.3.285.

Hack, N., and Lauer, W. V. (2014). Mesh-Mould: Robotically Fabricated Spatial Meshes as Reinforced Concrete Formwork. Architectural Design, 84(3), 44–53. DOI: https://doi.org/10.1002/ad.1753.

Hack, N., Dörfler, K., Walzer, A. N., Wangler, T., Mata-Falcón, J., Kumar, N., Buchli, J., Kaufmann, W., Flatt, R. J., Gramazio, F., and Kohler, M. (2020). Structural Stay-In-Place Formwork For Robotic In Situ Fabrication Of Non-Standard Concrete Structures: A Real Scale Architectural Demonstrator. Automation in Construction, 115 (2020), 103197. https://doi.org/10.1016/j.autcon.2020.103197.

Howe, A. S. (2000). Designing for automated construction. Automation in Construction, 9(3), 259–276. DOI: https://doi.org/10.1016/S0926-5805(99)00041-2.

Institute for Advanced Architecture of Catalonia, IAAC Barcelona. (2016). 3D printed bridge. Available online: www.iaac.net/project/3d-printed-bridge/ (accessed on May 8th, 2019).

ISO 17296–2:2015, Additive manufacturing—General principles Part 2: Overview of process categories and feedstock (2016), Standard, International Organization for Standardization, Geneva, CH.

ISO 17296–3:2016, Additive manufacturing—General principles Part 3: Main characteristics and corresponding test methods (2016), Standard, International Organization for Standardization, Geneva, CH.

Khoshnevis, B., Hwang, D., Yao, K., and Yeh, Z., (2006). Mega-scale fabrication by contour crafting. International Journal Industrial and Systems Engineering, 1(3), 301–320. DOI: https://doi.org/10.1504/IJISE.2006.009791.

Kolarevic, B. (2005). Architecture in the Digital Age: Design and Manufacturing, New York & London: Spon Press—Taylor & Francis Group, 308 p. ISBN: 978–0415381413.

Kristensen, M. K., and Raun, C. (2011). Patent WO2012065614 (A1): A flexible mat for providing a dynamically reconfigurable double-curved moulding surface in a mould.

Kuntse, H. B., Hirsch, U., Jacubasch, A., Eberle, F., and Goller, B. (1995). On the dynamic control of a hydraulic large range robot for construction applications. Automation in Construction, 4(1), 61–73. DOI: https://doi.org/10.1016/0926-5805(94)00036-M.

Labonnote, N., Rønnquist, A., Manum, B., and Rüther, P. (2016). Additive construction: State-of-the-art, challenges and opportunities. Automation in Construction, 72(3), 347–366. DOI: https://doi.org/10.1016/j.autcon.2016.08.026.

Latham, M. (1994). Constructing the Team, HMSO, London [PDF file]. Retrieved from: http://constructingexcellence.org.uk/wp-content/uploads/2014/10/Constructing-the-team-The-Latham-Report.pdf.

Le, T. T, Austin, S. A., Lim, S., Buswell, R. A., Law, R., Gibb, A. G. F., and Thorpe, T. (2012a). Hardened properties of high-performance printing concrete. Cement and Concrete Research, 42(3), 558–566. DOI: https://doi.org/10.1016/j.cemconres.2011.12.003.

Le, T. T, Austin, S. A, Lim, S., Buswell, R. A., Gibb, A. G. F., and Thorpe, T. (2012b). Mix design and fresh properties for high-performance printing concrete. Materials and Structures, 45(-), 1221–1232. DOI: https://doi.org/10.1617/s11527-012-9828-z.

Lim, S., Buswell, R., A., Le, T. T., Austin, S. A., Gibb, A. G. F., and Thorpe, T. (2012). Developments in construction-scale additive manufacturing processes. Automation in Construction, 21(-), 262–268. DOI: https://doi.org/10.1016/j.autcon.2011.06.010.

Lim, S, Buswell, R. A., Valentine, P. J., Piker, D., Austin, S., and De Kestelier, X. (2016). Modelling curved-layered printing paths for fabricating large-scale construction components. Additive Manufacturing, 12(Part B), 216–230. DOI: https://doi.org/10.1016/j.addma.2016.06.004.

Lipson, H., and Kurman, M., (2013). Fabricated: the New World of 3D Printing. John Wiley & Sons, Indianapolis, USA, 320 p. ISBN: 978–1–118–35063–8.

Lloret, E., Shahab, A., Mettler, L., Flatt, R. J., Gramazio, F., Kohler, M., and Langenberg, S. (2015). Complex concrete structures: Merging existing casting techniques with digital fabrication. Computer-Aided Design, 60(-), 40–49. DOI: https://doi.org/10.1016/j.cad.2014.02.011.

Lloret Fritschi, E. (2016). Smart Dynamic Casting—A digital fabrication method for non-standard concrete structures. (ETH Zurich) [PhD Thesis]. DOI: https://doi.org/10.3929/ethz-a-010800371.

Lloret Fritschi, E., Reiter, L., Wangler, T., Gramazio, F., Kohler, M., and R.J. Flatt, (2017). Smart Dynamic Casting: Slipforming with Flexible Formwork – Inline Measurement and Control. In *HPC/CIC Tromsø 2017*, *Norway, March 6–8* (Norwegian Concrete Association). DOI:https://doi.org/10.3929/ethz-b-000219663.

Lloret-Fritschi, E., Scotto, F., Gramazio, F., Kohler, M., Graser, K., Wangler, T., Reiter, L., Mata-Falcón, J., and Flatt, R. J. (2019) Challenges of Real-Scale Production with Smart Dynamic Casting. in First RILEM International Conference on Concrete and Digital Fabrication – Digital

Concrete 2018 (eds. Wangler, T. & Flatt, R. J.) pp. 299–310. Springer International Publishing. DOI: https://doi.org/10.1007/978-3-319-99519-9_28.

Lloret-Fritschil, E. Wangler, T. Gebhard, L., Mata-Falcón, J., Mantellato, S., Scotto, F. Burger, J., Szabo, A., Ruffray, N., Reiter, L., Boscaro, F., Kaufmann, W., Kohler, M., Gramazio, F., and Flatt, R. (2020). From Smart Dynamic Casting to a growing family of Digital Casting Systems. Cement and Concrete Research. 134(S.I.). DOI: https://doi.org/10.1016/j.cemconres.2020.106078.

Lowke, D., Dini, E., Perrot, A., Weger, D., Gehlen, C., and Dillenburger, B. (2018). Particle-bed 3D printing in concrete construction—possibilities and challenges. Cement and Concrete Research, 112(S.I.), 50–65. DOI: https://doi.org/10.1016/j.cemconres.2018.05.018.

Marchon, D., Kawashima, S., Bessaies-Bey, H., Mantellato, S., and Ng, S. (2018). Hydration and rheology control of concrete for digital fabrication: Potential admixtures and cement chemistry. Cement and Concrete Research, 112(S.I.), 96–110. DOI: https://doi.org/10.1016/j.cemconres.2018.05.014.

Mechtcherine, V., Nerella, V. N., Will, F., Näther, M., Otto, J., and Krause, M. (2019). Large-scale digital concrete construction – CONPrint3D concept for on-site, monolithic 3D-printing. Automation in Construction, 107(-), 102933. DOI: https://doi.org/10.1016/j.autcon.2019.102933.

Menges, A. (2006). Manufacturing diversity. Architectural Design, 76(2), 70–77. DOI: https://doi.org/10.1002/ad.242.

Mettler, L. K., Wittel, F. K., Flatt, R. J., and Herrmann, H. J. (2016). Evolution of strength and failure of SCC during early hydration. Cement and Concrete Research, 89(-), 288–296. DOI: https://doi.org/10.1016/j.cemconres.2016.09.004.

Nerella, V. N., Hempel, S., and Mechtcherine, V. (2019). Effects of layer-interface properties on mechanical performance of concrete elements produced by extrusion-based 3d-printing. Construction and Building Materials, 205(-), 586–601. DOI: https://doi.org/10.1016/j.conbuildmat.2019.01.235.

Neudecker, S., Bruns, C., Gerbers, R., Heyn, J., Dietrich, F., Dröder, K., and Kloft, H. (2016). A New Robotic Spray Technology for Generative Manufacturing of Complex Concrete Structures Without Formwork. Procedia CIRP, 43(-), 333–338. DOI: https://doi.org/10.1016/j.procir.2016.02.107.

Nolte, N., Heidmann-Ruhz, M., Krauss, H.-W., Varady, P., Budelmann, H., and Wolter, A. (2018). Development of shotcrete mixtures with controllable properties for the additive manufacturing of concrete structures. In: Prof. Wolfgang Kusterle (Ed.), Spritzbeton-Tagung. (pp. 1–13). Alpbach.

Pierre, A., Weger, D., Perrot, A., and Lowke, D. (2018). Penetration of cement pastes into sand packings during 3D printing: analytical and experimental study. Materials and Structures, 51(1), 22. https://doi.org/https://doi.org/10.1617/s11527-018-1148-5.

Raun, J. C., and Henriksen., Th. (2014). Patent 51403: Verfahren zur Herstellung eines flächenartigen Elements mit von einer ebenen Oberfläche abweichender Oberfläche, Formteil zur Herstellung eines derartigen flächenartigen Elements sowie flächenartiges Element.

Reiter, L., Wangler, T., Roussel, N., and Flatt, R. J. (2018). The role of early age structural build-up in digital fabrication with concrete. Cement and Concrete Research, 112(S.I.), 86–95. DOI: https://doi.org/10.1016/j.cemconres.2018.05.011.

Roussel, N. (2018). Rheological requirements for printable concretes. Cement and Concrete Research, 112(S.I.), 76–85. DOI: https://doi.org/10.1016/j.cemconres.2018.04.005.

Salet, T., Ahmed, Z., Bos, F., and Laagland, H. L. M. (2018). Design of a 3D printed concrete bridge by testing. Virtual and Physical Prototyping, 13(3), 222–236. DOI: https://doi.org/10.1080/17452759.2018.1476064.

Schipper, H. R., Grünewald, S., Eigenraam, P., Raghunath, P., and Kok., M. D. (2015a). Production of curved precast concrete elements for shell structures and free-form architecture using the flexible mould method. New Building Materials & Construction World, 20(8), 100–112.

Schipper, H. R., Eigenraam, P., Grünewald, S., Soru, M., Nap, P., van Overveld, B., and Vermeulen, J. (2015b). Kine-mould: Manufacturing technology for curved architectural elements in concrete. In: Jeroen Coenders, Andrew Borgart, and Arno Pronk, editors, Proceedings of the International Society Of Flexible Formwork (ISOFF) Symposium, Amsterdam. KIVI.

Schipper, H. R., and Eigenraam, P. (2016). Mapping double-curved surfaces for production as precast concrete shell elements. HERON, 61(3), 211–234 [PDF file]. Retrieved from: http://heronjournal.nl/61-3/6.pdf.

Schodek, D., Bechthold, M., Griggs, K., Kao, and Steinberg, M. (2005). Digital Design and manufacturing: CAD/CAM Applications in Architecture and Design, First ed, Wiley and Sons, Hoboken, New Jersey, p. 384. ISBN: 978–0471456360.

Siemens. (2017a). Made smarter review [PDF file]. Retrieved from: https://assets.publishing.service.gov.uk/government/uploads/system/uploads/attachment_data/file/655570/20171027_MadeSmarter_FINAL_DIGITAL.pdf.

Siemens. (2017b). Made smarter review. https://www.gov.uk/government/publications/made-smarter-review.

Tay, Y. W. D., Ting, G. H. A., Qian, Y., Panda, B., He, L., and Tan, M. J. (2019). Time gap effect on bond strength of 3D-printed concrete. Virtual and Physical Prototyping, 14(1), 104–113. DOI: https://doi.org/10.1080/17452759.2018.1500420.

Troughton, M. J. (2008). Mechanical fastening. In: Handbook of Plastics Joining, second edition, pp. 175–201. William Andrew Publishing (Chapter 8). ISBN 9780815515814, DOI: https://doi.org/10.1016/B978-0-8155-1581-4.50020-2.

Urschel, W. E. (1941). US2339892A. Machine for building walls [PDF file]. Retrieved from: https://patents.google.com/patent/US2339892.

Valencia, N. (2017). World's First 3D Printed Bridge Opens in Spain. Available online: www.archdaily.com/804596/worlds-first-3d-printed-bridge-opens-in-spain (Accessed on September 5th, 2019).

Vollers, K.J., and Rietbergen, D. (2010). Patent NL 2001738 (C2): Curved panel producing method, involves depositing viscous-liquid material on horizontal plane of mold, hardening viscous-liquid material, providing flexible material in mold, forming edge profile, and cutting profile at regular intervals.

Wolfs, R., Bos, F., and Salet, T. (2018a). Early age mechanical behaviour of 3D printed concrete: Numerical modelling and experimental testing. Cement and Concrete Research, 106, 103–116. https://doi.org/10.1016/j.cemconres.2018.02.001.

Wolfs, R. J., Bos, F. P., van Strien, E. C., and Salet, T. A. (2018b). A real-time height measurement and feedback system for 3D concrete printing. In High Tech Concrete: Where Technology and Engineering Meet, pp. 2474–2483. Springer, Cham. DOI: https://doi.org/10.1007/978-3-319-59471-2_282.

Wolfs, R., Bos, F., and Salet, T. (2018c). Correlation between destructive compression tests and non-destructive ultrasonic measurements on early age 3D printed concrete. Construction and Building Materials, 181(-), 447–454. DOI: https://doi.org/10.1016/j.conbuildmat.2018.06.060.

Wolfs, R. J. M., and Suiker, A. S. J. (2019a). Structural failure during extrusion-based 3D printing processes. International Journal of Advanced Manufacturing Technology, 104(-), 565–584. DOI: https://doi.org/10.1007/s00170-019-03844-6.

Wolfs, R., Bos, F., and Salet, T. (2019b). Hardened properties of 3D printed concrete: The influence of process parameters on interlayer adhesion. Cement and Concrete Research, 119(-), 132–140. DOI: https://doi.org/10.1016/j.cemconres.2019.02.017.

Yamazaki, Y., and Maeda, J. (1998). The SMART system: an integrated application of automation and information technology in production process. Computers in Industry, 35(1), 87–99. DOI: https://doi.org/10.1016/S0166-3615(97)00086-9.

Yamazaki, Y., and Maeda, J. (1998). The SMART system: an integrated application of automation and information technology in production process. Computers in Industry, 35, 87–99.